USING CAPACITORS IN PREDICTIVE CONDITION MONITORING OF LAMINATED POLYMER COMPOSITE BEARINGS

A. Rezaei[1*], P. Rombouts[2], W. Van Paepegem[1], P. De Baets[3], J. Degerick[1], L. Weyten[2]

[1]Department of materials science and engineering, Ghent University, Belgium
[2]Department of Electronics and information systems, Ghent University, Belgium
[3]Department of Mechanical construction and production, Ghent University, Belgium
**E-mail: ali.rezaei@ugent.be*

Keywords: condition monitoring, laminated composite, bearing.

Abstract

A new tool for predictive condition monitoring of laminated polymer composite bearings is developed. The tool is made of embedded capacitors between the layers of a laminated composite bearing. A laminated glass-epoxy composite bearing was made and two capacitors were embedded between the laminas. Two preliminary experiments were performed with an electromechanical testing machine. In the first experiment, a uniform pressure was applied all over the surface of the bearing, and in the second experiment, the pressure was applied on half of the bearing surface. During the experiments, variation of the capacitors' capacitance was measured versus the applied pressure. Besides the experiments, a simplified two-dimensional finite element model was built up and validated with the experiments. The results show that the variation of the capacitors corresponds to the stress distribution in the bearing.

1 Introduction

Condition monitoring is the process in which a parameter of machinery is monitored during its application. It is a modern way of controlling the operational safety in the machinery. Condition monitoring helps to schedule the maintenance of a system, and thereby preventing its failure before it happens. Indeed, monitoring the deviation of the monitored parameter from a reference value leads to identify and impede the possible damages [1].

Bearings are the most important items in the condition monitoring of rotating machinery. Measurement is usually performed at the points in which the shaft is supported with bearings, and the vibration generated by the bearing is analyzed concurrently. This kind of monitoring needs to analyze the vibration signals using methods like neural networks [2, 3]. There are also some other methods used for condition monitoring of rotating equipment, for instance: thermography, spectrographic oil analysis, ultrasound scan and visual inspection [4].

Laminated composite bearings are gaining more popularity in different machineries [5, 6]. Therefore, condition monitoring of these bearings will be an important requirement in the near future. By this time, there is no specific condition monitoring method for them. Potentially, parameters as temperature, deformation and stress can be important candidate parameters for monitoring of the laminated bearing's condition. Among these parameters, measuring the stresses is not a common method for condition monitoring (due to the technical difficulties). Nevertheless, by analyzing the stresses in a laminated bearing, one can detect whether the bearing is overloaded or not, and if it works in a proper condition or not.

In this article, a new tool for predictive condition monitoring of laminated composite bearings is developed. This tool consists of embedded capacitors between the layers of a laminated composite bearing. The basic idea is to use the capacitors as stress sensor in the bearing. This research is limited to a feasibility study of the calibration of the capacitors based on the compressive stresses in a laminated glass/epoxy composite. The idea benefits from a Wheatstone bridge for capacitance measurements, which potentially makes the method cheap and simple. The purpose of this article is introduction of the novelty of the method and its potential possibilities.

2 Principal of the idea

The principle of condition monitoring of laminated composite bearings is illustrated in figure 1. In this configuration, three copper foil electrodes (A-electrode, B-electrode and C-electrode) are embedded between the laminas of a composite bearing, according to the depicted arrangement. Supposing that the matrix and fibers of the composite material are not electrically conductive, the arrangement of the copper foils results in an equivalent circuit consisting of two sensing capacitors.

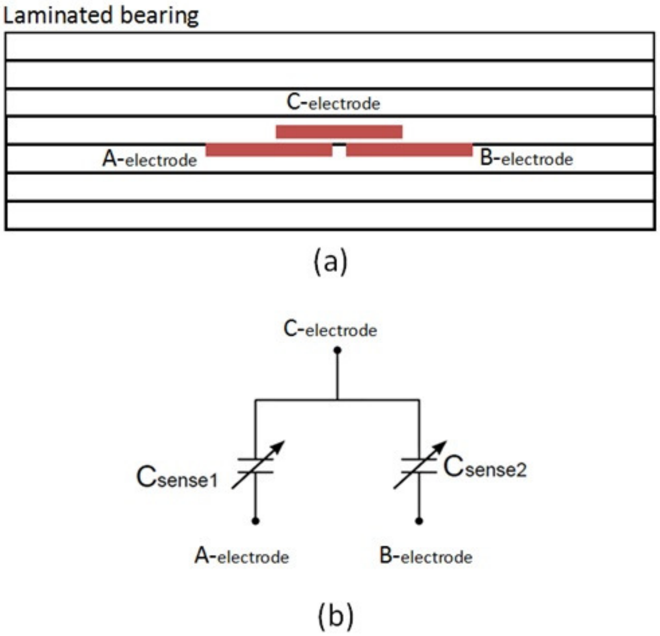

(a)

(b)

Figure 1. Basic concept of condition monitoring of laminated bearings: (a) Copper foils embedded between the composite laminas, (b) Equivalent circuit to the foils arrangement.

The idea is to use this configuration as a sensor to measure the stresses in the bearing. Here the average value of the two sensing capacitors will correspond to the compressive stresses since in this case both sensing capacitors C_{sense1} and C_{sense2} will vary in the same direction. The difference between the capacitance of the two sensing capacitors will correspond to the uneven compressive stresses since in this case both sensing capacitors (C_{sense1} and C_{sense2}) will vary in the opposite direction.

Based on the explained configuration in figure 1, a laminated glass-epoxy composite bearing was made, and three copper foils were embedded between the laminas (Figure 2). To make the bearing, the copper foils were attached to both sides of a paper ribbon (dielectric medium). This arrangement built up the sensing capacitors. Afterwards, the sensing capacitors were embedded between the fiberglass fabrics impregnated with a cold-curing epoxy resin. At the end, the assembly was placed inside a die to finalize the shape and curing process of the bearing. The dimensions of the bearing were 43.8 mm by 45.51 mm by 5.6 mm.

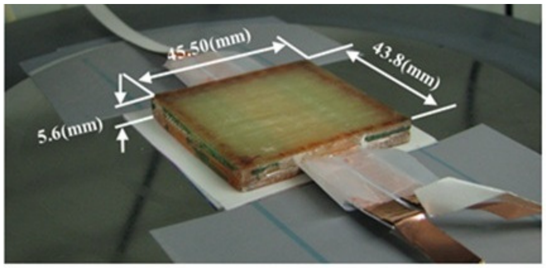

Figure 2. The sensor embedded glass-epoxy bearing

3 Experiments

Two preliminary experiments were performed to evaluate the practicality of the idea. The experiments were performed with an electromechanical testing machine. In the first experiment, a uniform pressure was applied all over the surface of the bearing (Test-A; symmetric loading). In the second experiment, the pressure was applied on half of the bearing surface (Test-B; asymmetric loading). Figure 3 shows the schematic diagram of the experiments.

In both experiments the load was applied gradually from 0.0 kN up to 2.0 kN and then it was released with the same rate. Each experiment was repeated three times, and the measurements were recorded with 100 kHz sampling frequency.

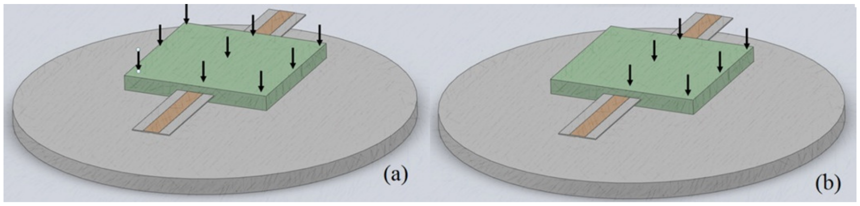

Figure 3. Schematic diagram of the performed experiments. (a) Test-A: symmetric loading, (b) Test-B: asymmetric loading.

Figure 4 depicts the results of the test-A. The sensing capacitors exhibited a variation of up to 0.55 pF in common mode. By increasing the load the average capacitance increases slowly, and by decreasing the load the average capacitance gradually decreases. The equivalent parallel conductance is small and shows a variation of up to 10%. Moreover, the overall equivalent parallel conductance is negative. The differential capacitance mode has a very small variation of up to 0.02 pF. The conductance variation for differential mode is very small about 3 %. Here also the overall equivalent parallel is negative.

Figure 5 depicts the measurement results of the test-B. The sensing capacitors exhibited a variation of up to 0.25 pF in common mode. Similar to the test-A the variation of the common mode capacitance directly corresponds to the load variation. However, the variation of the common mode capacitance is lower than test-A. In addition, the equivalent parallel conductance shows lower variation of up to 4%. Contrary to the test-A the differential capacitance shows a larger variation of up to 0.22 pF. The conductance variation for differential mode is very small about 3 %. As seen in both experiments the overall equivalent parallel conductance is negative, which indicates that the losses cannot be modeled by a simple parallel conductance mechanism.

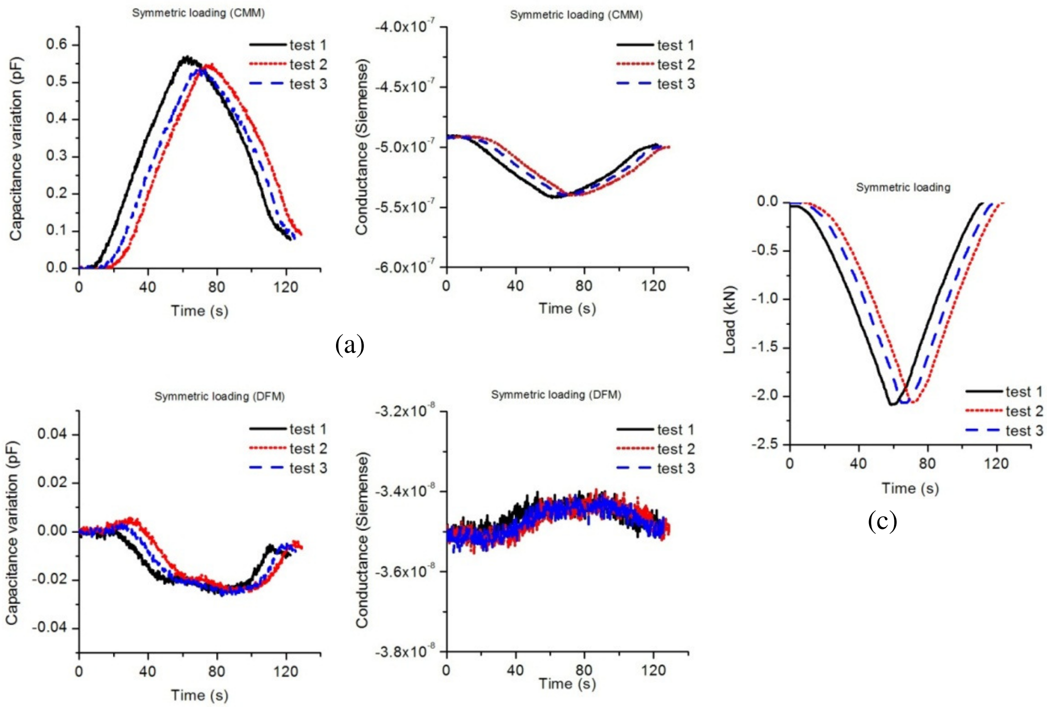

(a)

(c)

(b)

Figure 4. Measurement results of the test-A, in which the bearing was loaded symmetrically up to 2 kN. (a): Capacitance variation and parallel conductance variation for common mode, (b) Capacitance variation and parallel conductance variation for differential mode, (c): Loading rate

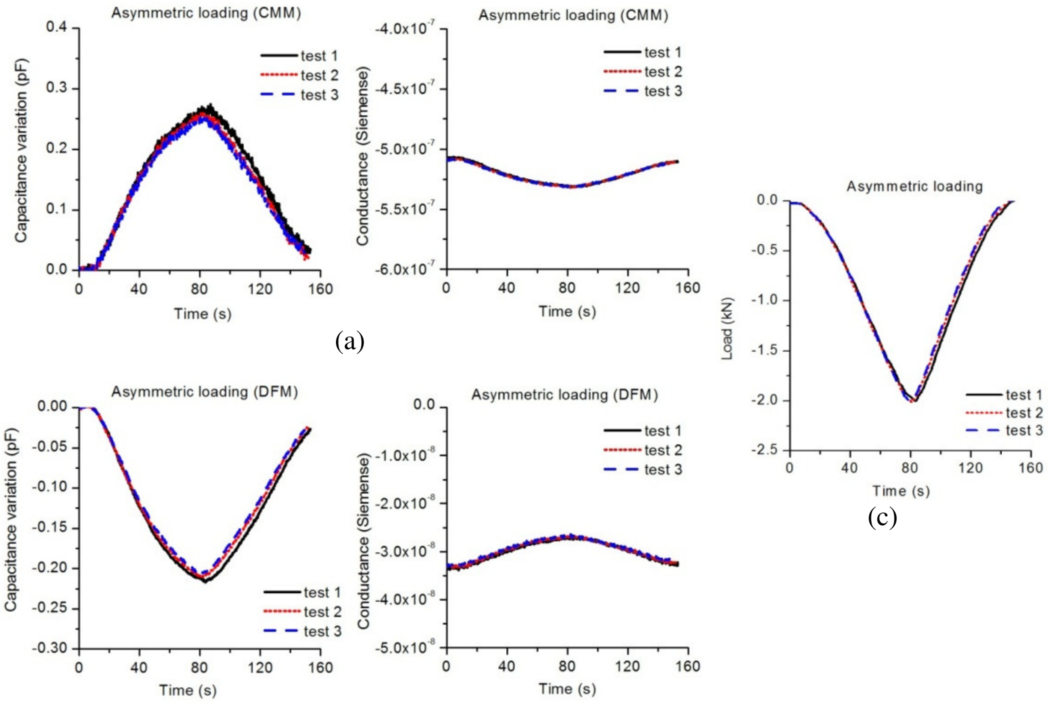

(a)

(c)

(b)

Figure 5. Measurement results of the test-B, in which the bearing was loaded asymmetrically up to 2 kN. (a): Capacitance variation and parallel conductance variation for common mode, (b) Capacitance variation and parallel conductance variation for differential mode, (c): Loading rate

4 Finite element simulation

The experiments were simulated using a simplified plane strain finite element model. Figure 6 illustrates the details of the boundary conditions and meshing of the finite element model. Followings are the conditions of the simulation:

- The finite element model was built up using ABAQUS package.
- The model was static; therefore the loading rate did not affect the results.
- About 40000 linear quadrilateral elements were used to discretize the bearing.
- The material properties were not measured and obtained from literature. Table 1 represents the material properties of the copper foils, paper, and bearing.

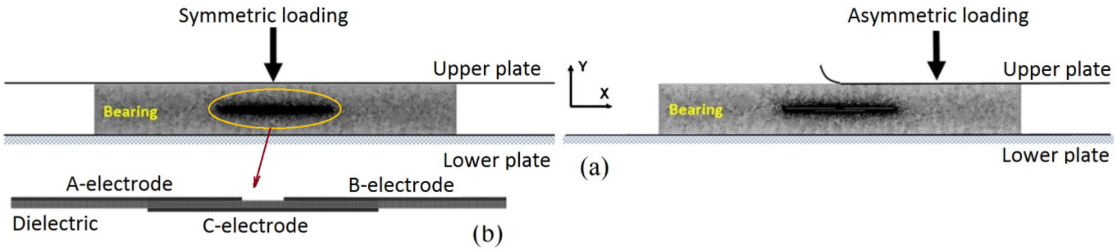

Figure 6. Finite element simulation of the sensor embedded laminated bearing. In the models, the upper and lower plates were rigid parts. The lower plate was fixed, and the load was applied on the upper plate. (a) Boundary condition of the model, (b) Meshing of the model.

The finite element model was coupled to a MATLAB program to calculate the capacitance variation of the sensing capacitors. The program was developed based on the parallel-plate capacitor theory in which the capacitance is obtained from the following relation [7]:

$$C = k\frac{\varepsilon_0 A}{d} \tag{1}$$

Where C is the capacitance of the capacitor (F), k is the relative permittivity of the dielectric (k=1 for vacuum, k>1 for all media, approximately =1 for air), ε_0 is the vacuum permittivity ($8.854*10^{-12}$ F/m), A is the conductor area (m^2), and d is the thickness of the dielectric (m).

		Glass-epoxy			
Copper		E_{11}	20	GPa	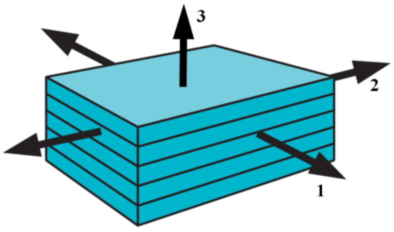
Young's modulus	117 GPa	E_{22}	20	GPa	
Poisson’s ratio	0.33	E_{33}	8.25	GPa	
Paper		υ_{12}	0.25		
Young's modulus	1 GPa	υ_{13}	0.16		
Poisson’s ratio	0.33	υ_{23}	0.16		
k (relative permittivity)	3.0	G_{12}	4	GPa	
		G_{13}	2	GPa	
		G_{23}	2	GPa	

Table 1: Material properties implemented in the simulations [8], [9], [10].

Figure 7 shows the discretization of the sensing capacitors in the simulation. In this figure, C_{sense1} and C_{sense2} are the two sensing capacitors. It is supposed that each sensing capacitor is a parallel arrangement of smaller capacitors C_1, C_2, …C_i. The total capacitor will then be calculated as below;

$$C = C_1 + C_2 + \cdots + C_i + \cdots C_n \tag{2}$$

In which C is the total capacitance and C_i is the capacitance of the small segments. In this configuration the conductor area A and dielectric thickness d of the capacitor C_i are:

$$A = |x(a_{i+1}) - x(a_i)| * t \tag{3}$$

$$d = \frac{\left|\left(x(b_{i+1}) - x(b_i)\right).\left(y(b_i) - y(a_i)\right) - \left(x(b_i) - x(a_i)\right).\left(y(b_{i+1}) - y(b_i)\right)\right|}{\sqrt{\left(x(b_{i+1}) - x(b_i)\right)^2 + \left(y(b_{i+1}) - y(b_i)\right)^2}} \tag{4}$$

Where $x(a_i)$ and $y(a_i)$ denote the Cartesian coordinates of the node a_i, *and* t is the width of the capacitor (in the plane strain model t=1).

Solving the finite element model, the displacements of the boundary nodes of the C_{sense1} and C_{sense2} are recorded and thereby the capacitance of each segment was calculated based on equation 1.

Figure 8 represents the variation of the common mode and differential mode for the test-A and test-B. For the test-A the common mode varies about 0.025 pF, and the differential mode does not change. For the test-B the common mode changes about 0.021 pF, and the differential mode varies about 0.025 pF. The simulation results are almost one tenth of the experiments. Several reasons may explain the discrepancy of the simulations and the experiments.

The bearing is handmade; therefore, some imperfections are expected in the bearing. For instance, microscopic analyses (figure 9) reveal that at the corners of the capacitors, epoxy diffuses between the copper foils and the paper. In addition, there is a thin layer of glue between the copper foils and the paper that can change permittivity of the paper. There are also some deformations in the capacitors during the fabrication. These issues can severely affect the capacitance of the sensors.

The parallel plate theory cannot be a flawless model for these capacitors since the electric fields at the corners of the copper foils are very complex [11].

While the quantity of the experimental measurements and numerical calculations do not correspond very well, the behavior of the capacitors was similar in the simulations and experiments. This confirms that the variation of the capacitors corresponds to the stress distribution in the bearing. The results indicate that the stress distribution in the bearing can be calibrated in relation to the capacitance variation in the capacitors.

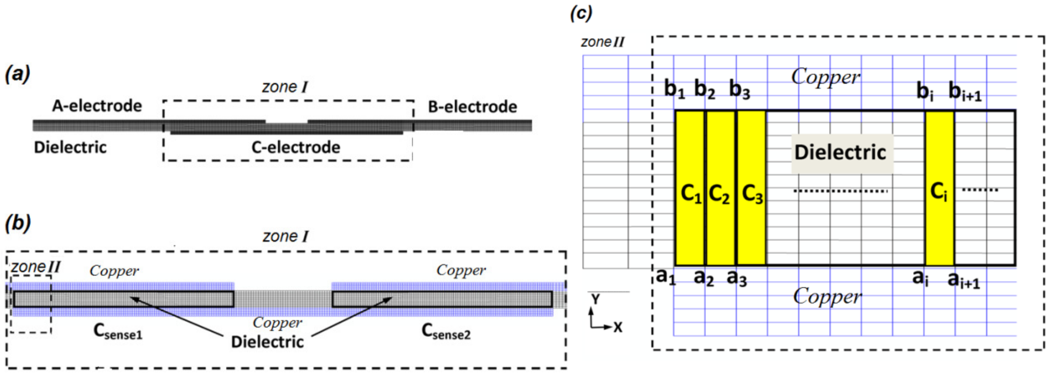

Figure 7. Finite element discretization of the capacitors. (a): Arrangement of the electrodes and dielectric, (b): Magnification of the zone I which includes the sensing capacitors Csense1 and Csense2, (c): Magnification of the zone II including the parallel arrangement of small capacitors (C1, C2 …Ci)

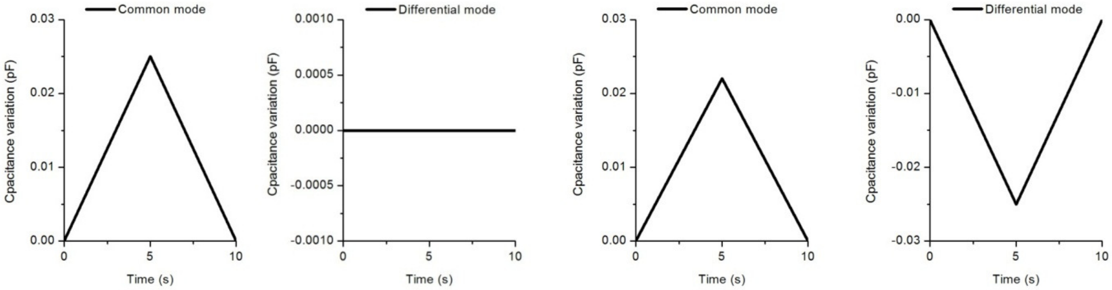

(a) (b)

Figure 8. Finite element simulation results. Variation of the common mode and differential mode. (a): the test-A (symmetric loading) and (b) test-B (asymmetric loading).

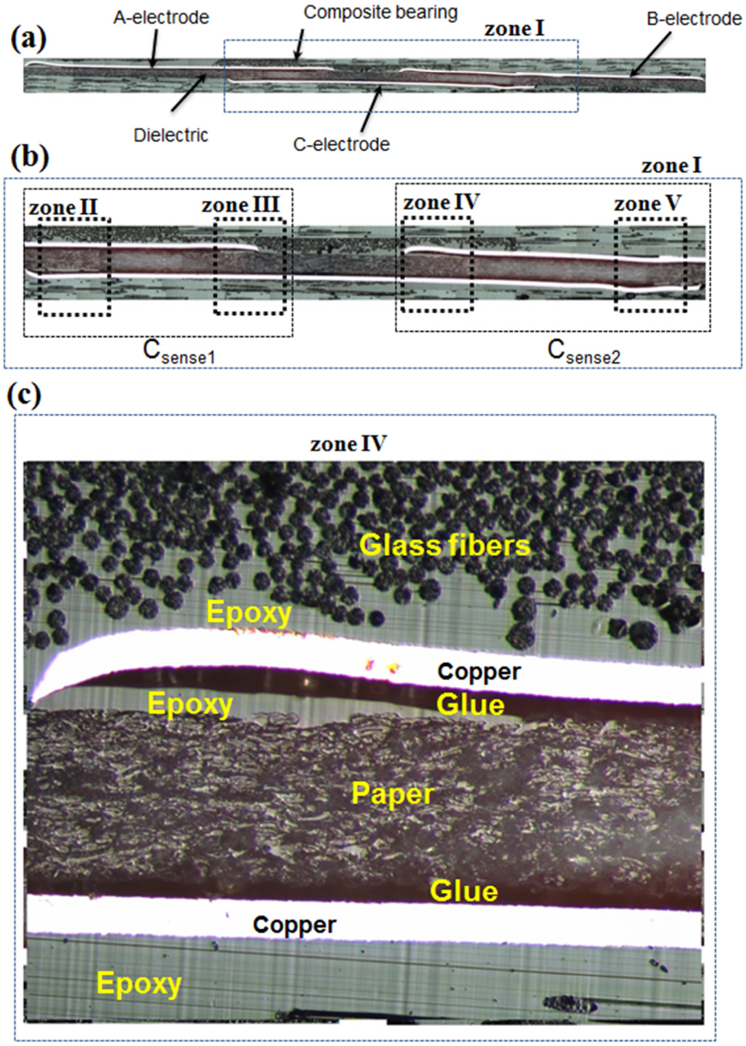

Figure 9. Microscopy of the capacitor's section. (a): Polished segment of the bearing. Arrangement of the capacitors, electrodes, dielectric (paper) and composite material is shown. (b): Magnification of the zone I. Capacitors C_{sense1} and C_{sense2} are shown. Zone II, III, IV and V represent some imperfections in the capacitors. (c): Magnification of the zone IV. Deformation of the corner of the copper foil, diffusion of epoxy between the copper foil and paper, and a thin layer of glue between the paper and the copper are observed.

5 Conclusion

A new Condition monitoring tool for laminated composite bearings was developed. The basic idea was to use the capacitors as pressure sensor in the bearing. The idea was evaluated with preliminary experiments on a glass-epoxy bearing. In addition, a simplified finite element model was made to simulate the variation of the sensing capacitors in relation to the applied pressure on the bearing. As was expected when the pressure is symmetrically distributed on the bearing the common mode of the capacitors changes more than the differential mode. In the asymmetric loading, the differential mode also changes considerably. In summary, the performed experiments and simulations show that the variation of the capacitors corresponds to the pressure on the bearing. Conceptually, measuring the stress level of laminated bearings using embedded capacitors can help to provide a simple, cheap and direct condition monitoring method. However further studies are required to find a practical model to calibrate the bearing's stress with the capacitors. It is necessary to improve the quality of the bearing and capacitors to arrange better experiments. In addition, it is required that the capacitors be simulated with more advanced theories.

References

[1] Miettinen, J. *Condition monitoring of grease lubricated rolling bearings by acoustic emission measurements*, in Laboratory of Machine Dynamics. Tampere University of Technology, Finland (2000).

[2] Tandon, N. A comparison of some vibration parameters for the condition monitoring of rolling element bearings. *Measurement*. **12**, pp. 285-289 (1994).

[3] Samanta, B. and K.R. Al-Balushi. Artificial neural network based fault diagnostics of rolling element bearings using time-domain features. *Mechanical Systems and Signal Processing*. **17**, pp. 317-328 (2003).

[4] Pusey, H.C. and P.L. Howard. *An Historical View of Mechanical Failure Prevention Technology*. Acoustical Publications, Cleveland, OH, ETATS-UNIS (2008).

[5] Rezaei, A., et al. Experimental study and numerical simulation of the large-scale testing of polymeric composite journal bearings: two-dimensional modeling and validation. *Tribology Letters*. **37**, pp. 12 (2009).

[6] Rezaei, A., et al. Experimental study and numerical simulation of the large-scale testing of polymeric composite journal bearings: Three-dimensional and dynamic modeling. *Wear*. **270**, pp. 431-438 (2011).

[7] Halliday, D., R. Resnick, and J. Walker. *Fundamentals of Physics*. John Wiley and Sons, US (2010).

[8] *Young's modulus*. Wikipedia, (cited 2010 December); Available from: http://en.wikipedia.org/wiki/Young's_modulus.

[9] *Young's Modulus - Density*. University of Cambridge, (cited 2010 December); Available from: http://www-materials.eng.cam.ac.uk/mpsite/interactive_charts/stiffness-cost/basic.html.

[10] *Permittivity: Dielectric constants of useful materials*. HvWiki, (cited 2010 December); Available from: http://wiki.4hv.org/index.php/Permittivity.

[11] Xiang, Y. The electrostatic capacitance of an inclined plate capacitor. *Journal of Electrostatics*. **64**, pp. 29-34 (2006).